VARIATION OF EIGENVALUES OF A HPC MOTOR SPINDLE DUE TO CHANGING AXIAL DEPTH OF CUT

B. Späh, S. Kern, R. Nordmann
Mechatronics in Mechanical Engineering
Technische Universität Darmstadt, Germany

e-mail:spaeh@mim.tu-darmstadt.de

The influence of the milling-process on the system-dynamics of a hybrid bearing HPC (high performance cutting) motor spindle is investigated. An additional electromagnetic actuator allows for identification and active vibration control. Semi-discretization is used to calculate the eigenvalues of the motor spindle depending on increasing axial depth of cut. This result is used to design a controller for chatter suppression that accounts for the influence of the process on the system dynamics. The controller increases the critical depth of cut considerably. The results of the semi-discretization as well as the effect of the active damping are validated by experimental identification during slot-milling of aluminum.

Keywords
milling, chatter-suppression, active vibration control, semi-discretization

1. Introduction

Chatter vibrations caused by the regenerative effect have been in the focus of research since the beginning of the 1960s. Main focus is the prediction of system stability and the calculation of stability lobe diagrams. Models of the cutting process are presented which mainly differ in description of the geometry of workpiece and tool, modeling of the process force and simplifications for the stability analysis [Weck 2006, Faasen 2007, Ganguli 2005].

One approach to improve process stability is active vibration control. There exist approaches using active work-piece mounts [Haase 2005], active vibration via active reaction mass dampers [Scandella 2004], piezo-supported ball bearings [Ries 2006] and fully magnetically levitated spindles [Stephens 1996]. Here an electromagnetic actuator is used for active damping of a motor spindle. The limited dynamics of the actuator prohibit the use of simple control laws and model based controller design is necessary. In this paper semi-discretization and a simple model of the milling process is used to show the influence of the milling process on the spindle-dynamics. Experimental identification is used to validate this result. Finally a controller is designed which is robust to the varying system dynamics under process conditions.

Figure 1 shows a drawing of the used motor spindle. It is mounted horizontally on a milling machine. An electromagnetic actuator is integrated, which is located between the front ball bearing and the milling tool. The actuator has the design of an 8-pole radial active magnetic bearing with a rotor diameter of 106 mm and maximum current of 15 A. Its maximum static force is approx. 800 N and the current control bandwidth is 1 kHz. This actuator serves for identification and control. In order to measure the radial deflection of the spindle two orthogonally oriented eddy-current sensors are integrated in front of the actuator. The tool used for this investigation is an end mill cutter with two flutes (***N***=2), a helix-angle of 45° and a diameter of 20 mm.

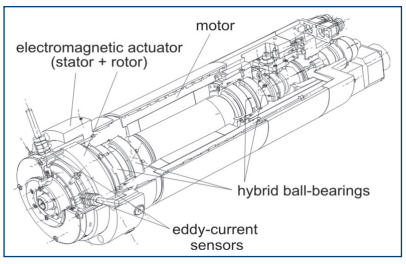

Figure 1. *Drawing of motor spindle.*

2. Milling process

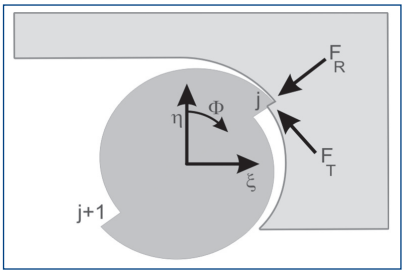

Figure 2. *Schematic of milling.*

The process is modeled for slot-milling along the ξ-direction in aluminium with the mentioned tool. A schematic representation is shown in Figure 2.

The process forces are modeled in the following way [Weck 2006, Faasen 2007]:

$$\begin{bmatrix} F_{R,j} \\ F_{T,j} \end{bmatrix} = b\,h(t) \begin{bmatrix} K_R \\ K_T \end{bmatrix}. \tag{2.1}$$

The radial and tangential forces $\boldsymbol{F_R}$ and $\boldsymbol{F_T}$ are proportional to the axial depth of cut $\boldsymbol{b}$ and the radial chip-thickness $\boldsymbol{h(t)}$.

The chip-thickness consists of two parts: one due to the feed (static), the other one due to periodic oscillations of the tool (dynamic). The oscillations are selfexcited by the regenerative effect. This is discussed among others in **[Altintas 1995, Insperger 2000]**. For stability-investigations only the regenerative effect is considered. Therfore only the dynamic part is of interest and the radial chip-thickness can be defined as

$$h(t) = \begin{bmatrix} \sin[\Phi_j(t)] & \cos[\Phi_j(t)] \end{bmatrix} \begin{bmatrix} \xi(t) - \xi(t-\tau) \\ \eta(t) - \eta(t-\tau) \end{bmatrix}, \tag{2.2}$$

where $\Phi_j(t)$ is the time-dependent actual angular position of the *j*th tooth. $\xi(t)$ and $\eta(t)$ describe the position of the tool at the time *t*. The position of the tool during the previous cut is described by $\xi(t-\tau)$ and $\eta(t-\tau)$ which leads to the chip-thicknesses in ξ- and η-direction: $\Delta\xi = \xi(t) - \xi(t-\tau)$ and $\Delta\eta = \eta(t) - \eta(t-\tau)$. The cutting coefficients in radial and tangential direction K_R and K_T have been determined experimentally. [Späch 2008]For the remainder of this paper the forces in ξ- and η -direction are of interest. Thus the forces are transformed and summed over all N teeth:

$$\begin{bmatrix} F_\xi \\ F_\eta \end{bmatrix} = \sum_{j=1}^{N} \begin{bmatrix} -\sin(\Phi_j) & -\cos(\Phi_j) \\ -\cos(\Phi_j) & \sin(\Phi_j) \end{bmatrix} \begin{bmatrix} F_{R,j} \\ F_{T,j} \end{bmatrix}. \tag{2.3}$$

With Eq. (2.1) and (2.2) this leads to:

$$\begin{bmatrix} F_\xi \\ F_\eta \end{bmatrix} = b \underbrace{\begin{bmatrix} K_{11} & K_{12} \\ K_{21} & K_{22} \end{bmatrix}}_{\boldsymbol{K}(\Phi)} \underbrace{\begin{bmatrix} \xi(t) - \xi(t-\tau) \\ \eta(t) - \eta(t-\tau) \end{bmatrix}}_{\boldsymbol{y}(t) - \boldsymbol{y}(t-\tau)} = b\,\boldsymbol{K}(\Phi)\big(\boldsymbol{y}(t) - \boldsymbol{y}(t-\tau)\big) \tag{2.4}$$

The elements of the $\boldsymbol{K}$- Matrix are

$$
\begin{aligned}
K_{11}(\Phi) &= \sum_{j=1}^{N}[-K_T\cos(\Phi_j)\sin(\Phi_j) - K_R\sin^2(\Phi_j)]g(\Phi_j)\\
K_{12}(\Phi) &= \sum_{j=1}^{N}[-K_T\cos^2(\Phi_j) - K_R\cos(\Phi_j)\sin(\Phi_j)]g(\Phi_j)\\
K_{21}(\Phi) &= \sum_{j=1}^{N}[K_T\sin^2(\Phi_j) - K_R\sin(\Phi_j)\cos(\Phi_j)]g(\Phi_j)\\
K_{22}(\Phi) &= \sum_{j=1}^{N}[K_T\cos(\Phi_j)\sin(\Phi_j) - K_R\cos^2(\Phi_j)]g(\Phi_j)
\end{aligned}
\qquad (2.5)
$$

where

$$
g(\Phi_j)=\begin{cases}1 & \text{for tooth in contact}\\ 0 & \text{tooth not in contact}\end{cases}. \qquad (2.6)
$$

In order to set up a complete model of the process not only the forces but also a model of the spindle-dynamics itself is needed. In this case the compliance of the spindel at the tip of the milling--tool is of interest. Since it is neither possible to excite nor to measure a displacement properly at a real milling tool, a dummy--tool with similar geometrical dimensions is needed. To identify the compliance frequency response in ξ- and η- direction, the dummy-tool is excited at its tip in both directions with an impulse hammer during idle run. The respective deformations are measured using laser-sensors. For these measurements a 2x2-model is fitted manually. Here the emphasis lies on an accurate fit in the frequency-range of the first resonance, since the chatter-frequency is found to be in this band.

The model

$$
\begin{aligned}
\dot{\boldsymbol{x}}(t) &= \boldsymbol{A}\boldsymbol{x}(t) + \boldsymbol{B}\boldsymbol{u}(t)\\
\boldsymbol{y}(t) &= \boldsymbol{C}\boldsymbol{x}(t)
\end{aligned}
\qquad (2.7)
$$

describes the deflection of the tool-tip in ξ- and η-direction. The state-space model is of 4th order and the two directions are coupled by gyroscopic effects:

Output $\boldsymbol{y}(t)$ are the deflections of the tool tip and input $\boldsymbol{u}(t)$ are the forces on the tool-tip:

$$
\boldsymbol{y}(t)=[\xi(t)\quad \eta(t)]^T \quad \text{and} \quad \boldsymbol{u}(t)=[F_\xi \quad F_\eta]^T. \qquad (2.8)
$$

Bodediagrams, i.e. dynamic compliance, of the system is shown in Figure 3. The discrepancy between measurements and modell especially in the coupling terms are due to small amplitudes and thus a bad coherence in these bands. In the relevant band of the dominant resonance the model matches the measurements well. Due to the anisotropic mounting of the spindle on the machine tool the dynamics is different in ξ- and η-direction. The modal parameters of the model are given in Table 1.

	1st mode	2nd mode
f_0 (Hz)	535	554
D (%)	1.2	1.2

Table. *Modal parameters of the spindle.*

Combination of the mechanical model (2.7) with the cutting force model (2.4) results in the system

$$
\begin{aligned}
\dot{\boldsymbol{x}}(t) &= \boldsymbol{A}\,\boldsymbol{x}(t) + \boldsymbol{B}\,b\,\boldsymbol{K}(\Phi)\big[\boldsymbol{y}(t) - \boldsymbol{y}(t-\tau)\big]\\
\boldsymbol{y}(t) &= \boldsymbol{C}\,\boldsymbol{x}(t)
\end{aligned}
\qquad (2.9)
$$

and after simplification in

$$
\begin{aligned}
\dot{\boldsymbol{x}}(t) &= \big[\boldsymbol{A} + \boldsymbol{B}\,b\,\boldsymbol{K}(\Phi)\boldsymbol{C}\big]\boldsymbol{x}(t) + \boldsymbol{B}\,b\,\boldsymbol{K}(\Phi)\boldsymbol{C}\,\boldsymbol{x}(t-\tau)\\
\boldsymbol{y}(t) &= \boldsymbol{C}\,\boldsymbol{x}(t).
\end{aligned}
\qquad (2.10)
$$

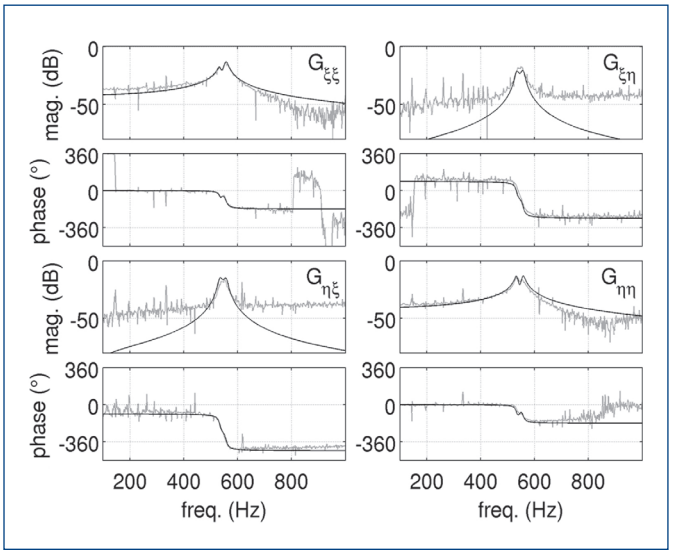

Figure 3. *Measured and modeled compliance of spindle (magnitude in µm/N).*

3. Semi-discretization

The semi-discretization is used to analyze the influence of increasing axial depth of cut on the eigenvalues of the milling-spindle. It was used by [Insperger 2002, Gradisek 2005] to calculate stability-lobe-diagrams for milling. In this paper the semi-discretization is applied only to a single spindle speed Ω of 20000 rpm. The milling process is periodic by the tooth-passing-frequency $\frac{1}{\tau}$, where $\tau=\frac{60}{\Omega N}$. Therefore it is sufficient to consider only one period for the stability investigation. For the semi-discretization such a period with length τ is divided into m intervals $[t_i, t_{i+1})$ of length Δt with

$$
\tau = m\cdot\Delta t, \quad m\in\mathbb{N} \qquad (3.1)
$$

and

$$
\Delta t = t_{i+1} - t_i, \quad i = 0,1,\ldots,m-1.
$$

The system is averaged for each interval by assuming $\boldsymbol{K}(\Phi)$ to be constant within such an intervall:

$$
\boldsymbol{K}(\Phi(t))\approx\boldsymbol{K}(\Phi(t_i))=:\boldsymbol{K}_i \qquad ,t\in[t_i, t_{i+1}). \qquad (3.2)
$$

Since the process is periodic to the time base τ, the state of the system i at the time $(t-\tau)$ is equal to the state of the system $i-m$ at time t:

$$
\boldsymbol{x}_i(t-\tau)=\boldsymbol{x}_{i-m}(t) \qquad ,t\in[t_i, t_{i+1}). \qquad (3.3)
$$

Assuming Δt to be sufficiently small the states can be taken as constant within the interval i and are approximated to:

$$
\begin{aligned}
\boldsymbol{x}(t-\tau) &\approx \frac{1}{2}\big[\boldsymbol{x}(t_{i-m}) + \boldsymbol{x}(t_{i-m+1})\big] \qquad ,t\in[t_i, t_{i+1})\\
&=: \frac{1}{2}\big[\boldsymbol{x}_{i-m} + \boldsymbol{x}_{i-m+1}\big].
\end{aligned}
\qquad (3.4)
$$

With these assumptions the systems result in

$$
\begin{aligned}
\dot{\boldsymbol{x}}_i(t) &= \big[\boldsymbol{A} + \boldsymbol{B}\,b\,\boldsymbol{K}_i\,\boldsymbol{C}\big]\boldsymbol{x}_i(t) + \frac{b}{2}\boldsymbol{B}\,\boldsymbol{K}_i\,\boldsymbol{C}\big(\boldsymbol{x}_{i-m} + \boldsymbol{x}_{i-m+1}\big)\\
\boldsymbol{y}_i(t) &= \boldsymbol{C}\boldsymbol{x}_i(t).
\end{aligned}
\qquad (3.5)
$$

For each of these m intervals the only unknowns in the state equation are $\dot{\boldsymbol{x}}_i(t)$ and $\boldsymbol{x}_i(t)$. Thus a solution of $\boldsymbol{x}(t)$ depending on $\boldsymbol{x}(t_0)$ can be found where $\boldsymbol{x}(t_0)$ equals the states at the left side and $\boldsymbol{x}(t)$ the states at the right side of each interval [Lutz 2003]:

$$
\begin{aligned}
\boldsymbol{x}(t_0) &= \boldsymbol{x}_i\\
\boldsymbol{x}(t) &= \boldsymbol{x}_{i+1}.
\end{aligned}
\qquad (3.6)
$$

$$\begin{aligned} \boldsymbol{x}_{i+1} &= e^{\boldsymbol{A}_i\cdot(t_{i+1}-t_i)}\left[\boldsymbol{x}_i + \boldsymbol{A}_i^{-1}\boldsymbol{B}_i\left(\boldsymbol{x}_{i-m}+\boldsymbol{x}_{i-m+1}\right)\right]- \\ &\quad \boldsymbol{A}_i^{-1}\boldsymbol{B}_i\left(\boldsymbol{x}_{i-m}+\boldsymbol{x}_{i-m+1}\right) \\ &= e^{\boldsymbol{A}_i\Delta t}\boldsymbol{x}_i + \left(e^{\boldsymbol{A}_i\Delta t} - \boldsymbol{I}\right)\boldsymbol{A}_i^{-1}\boldsymbol{B}_i\left(\boldsymbol{x}_{i-m}+\boldsymbol{x}_{i-m+1}\right) \\ &= \boldsymbol{P}_i\boldsymbol{x}_i + \boldsymbol{Q}_i\left(\boldsymbol{x}_{i-m}+\boldsymbol{x}_{i-m+1}\right). \end{aligned} \tag{3.7}$$

For each interval Eq.(3.7) can be rewritten considering the states of all *m* intervals:

$$\boldsymbol{x}_{i+1}^* = \boldsymbol{A}_i^*\boldsymbol{x}_i^* \quad \text{, with}$$

$$\boldsymbol{A}_i^* = \begin{bmatrix} \boldsymbol{P}_i & \boldsymbol{0} & \boldsymbol{0} & \cdots & \boldsymbol{0} & \boldsymbol{Q}_i & \boldsymbol{Q}_i \\ \boldsymbol{I} & \boldsymbol{0} & \boldsymbol{0} & \cdots & \boldsymbol{0} & \boldsymbol{0} & \boldsymbol{0} \\ \boldsymbol{0} & \boldsymbol{I} & \boldsymbol{0} & \cdots & \boldsymbol{0} & \boldsymbol{0} & \boldsymbol{0} \\ \vdots & \vdots & \vdots & \ddots & \vdots & \vdots & \vdots \\ \boldsymbol{0} & \boldsymbol{0} & \boldsymbol{0} & \cdots & \boldsymbol{I} & \boldsymbol{0} & \boldsymbol{0} \\ \boldsymbol{0} & \boldsymbol{0} & \boldsymbol{0} & \cdots & \boldsymbol{0} & \boldsymbol{I} & \boldsymbol{0} \end{bmatrix} \quad \text{and} \tag{3.8}$$

$$\boldsymbol{x}_i^* = \left[\boldsymbol{x}_i \;\; \boldsymbol{x}_{i-1} \;\; \boldsymbol{x}_{i-2} \;\; \cdots \;\; \boldsymbol{x}_{i-m+1} \;\; \boldsymbol{x}_{i-m}\right]^{\mathrm{T}}.$$

Combination of all *m* intervals leads to

$$\boldsymbol{x}_m = \Theta\,\boldsymbol{x}_0 \quad \text{with} \quad \Theta = A_{m-1}^*\cdot A_{m-2}^*\cdot\ldots\cdot A_1^*\cdot A_0^*. \tag{3.9}$$

System stability during the milling process can be observed by calculating the eigenvalues of Θ.

This procedure is repeated for every interesting depth of cut until the absolute value of an eigenvalue is greater than one and the system becomes instable.

3.1. Results of semi-discretization

The results of the semi-discretization are eigenvalues in dependency of the depth of cut. Due to the discretization they appear in the z-plane. Additional to the eigenvalues of the mechanical system eigenvalues close to zero appear. They do not have a physical meaning, but are caused by the discretization. The discretization-time ***T*** equals the inverse of the tooth-passing-frequency τ. This leads to problems when interpreting the position of the eigenvalues in the z-plane, where only frequencies up to π/τ are plotted correctly. Due to aliasing effects higher frequencies are mirrored on negative and lower frequencies. This is shown exemplary for frequencies up to 5000 Hz with ***D***=15 % in Figure 4.

At a spindle speed of 20000 rpm and 2 teeth, τ equals 1.5 ms. Thus frequencies up to 333 Hz are displayed correctly. Higher frequencies can be transformed into the Laplace-plane nonetheless:

$$\omega_0^2 = -\left\{\frac{\sqrt{-1}\left[\arg(z)+n\pi\right]}{T}\right\}^2 + \left(\frac{\ln|z|}{-T}\right)^2 \qquad n\in\mathbb{N} \tag{3.10}$$

$$D = \frac{\ln|z|}{-T\omega_0}. \tag{3.11}$$

Since the eigenfrequencies of the spindle during idle running are known, the factor ***n*** can be found iteratively. It has to be fitted in such a way that the eigenvalues in the Laplace-plane equal the eigenvalues of the model of the spindle during idle running. For increasing depth of cut the eigenvalues which are closest to the one calculated for the next smaller depth of cut are taken. The results for the considered system are shown in Figure 5 and 6. It shows that for this particular system the milling-process results in a slight change of frequency and damping for the considered eigenvalues. With increasing axial depth of cut the resonance-frequencies diverge: both frequencies increase but the higher one considerably faster than the lower one. The according damping-values increase and decrease respectively (cp. Figure 6). It can be seen that the damping-value of the lower frequency is reduced faster than the other one. Thus this frequency is the one which destabilizes the system first.

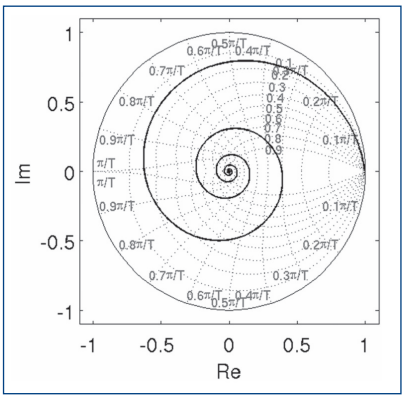

Figure 4. *Increasing frequencies with D=15% in z-plane.*

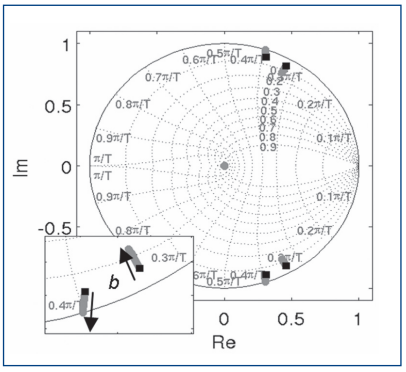

Figure 5. *Eigenvalues of spindle with increasing depth of cut in z-plane (T = τ). (Eigenvalues of idle spindle: black squares, eigenvalues of θ with increasing b: grey circles).*

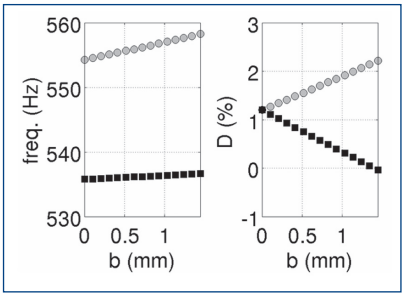

Figure 6. *Changing natural frequency and modal damping with increasing depth of cut.*

4. Measurements

The results of the theoretical analysis via semi-discretization are validated by experimental system identification during milling. The spindle is excited via the magnetic actuator and the deflection is measured by the eddy current position sensors. For excitation a sine-chirp signal is used as reference-signal for either ξ- or η-direction of the actuator. The amplitude is constant and the frequency varies between 50 Hz and 1200 Hz. The frequency response function (FRF) from spindle deflection to set current is calculated using Welch's method [Welch 1967].

The cutting forces result in significant deflections of the spindle during milling. Depending on the depth of cut these disturbances have higher amplitude than the excitation signal for identification. Nonetheless the identification gives good results in a broad frequency range: the process forces are periodic and consist only of harmonic components of the tooth-passing-frequency and its multiples. They are uncorrelated to the excitation signal in the frequency-ranges in-between.

The actuator force is proportional to the current in the coils. Since the bandwidth of the current-control of the actuator is approx. 1 kHz

and eddy-current losses are insignificant, the actuator force is proportional to the set current in the frequency range of the resonances, i.e. the frequency range of interest. So the identified FRFs are proportional to the spindles compliance at the actuators axial position.

The theoretical analysis shows that the eigenvalues of the spindle are changed by the process. Since eigenvalues are system-properties, this change of natural frequencies and damping can not only be seen in the resonances of the tool-tip compliance but also in the resonances of the compliance of the spindle at the position of the actuator..

Figure 7 shows FRFs that are identified during slot milling of aluminum at 20000 rpm with a 20 mm diameter two-fluted milling cutter. The depth of cut varies from 0 mm (idle run) to 1.5 mm. The FRFs show the system dynamics in feed-direction (ξ-direction). For all depths of cut the identification gives good results in the frequency range of the first two dominant resonances at approx. 550 Hz. The disturbances at 666 Hz that corresponds to the tooth passing frequency result from the process forces.

There are two resonances, one at 534 Hz and one at 555 Hz. Both correspond to the first bending-mode of the spindle. The anisotropic mount of the spindle and the gyroscopic effect are reasons for the splitting of these frequencies. With rising depth of cut b the damping of the first resonance decreases. This can be seen by the higher resonance-amplitude as well as by the steeper phase-drop in this frequency range. The system becomes instable at b slightly above 1.5 mm (not shown here). The damping of the second resonance increases with rising b and the resonance frequency moves from 555 Hz to 560 Hz. This behavior is identical to the predicted behavior that is shown in Figure 6.

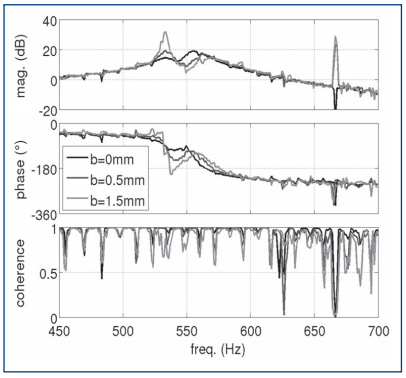

Figure 7. *Compliance of spindle at sensor position during milling. Excited by electromagnetic actuator. (Position/actuator variable)*

5. Active damping

In order to achieve stable operation at increased depths of cut and thus more efficient milling, active damping is applied to the spindle. As shown in [Ganguli 2005] regenerative chatter can be reduced by increased damping of the spindle-resonances. Using the integrated electromagnetic actuator active vibration control is applied. For this purpose a controller is designed that damps the first resonance considerably.

Unfortunately the control could only be tested with the spindle mounted on a different milling machine. This is why the dynamic compliance of the spindle is different (see Figure 8) as shown above. The main result of the previous sections, the change of the natural frequencies by approx. 10 Hz and the decreased damping during cutting, can be used for the controller design nonetheless.

The control loop consists of the actuator, the eddy current sensors and a dSPACE real time system. Control value is the measured deflection, actuating variable is the reference current of the amplifiers. The real-time system is sampled at 10 kHz.

A lead-lag-controller was tuned manually to achieve significant damping of the dominant resonance. Basis for this control design is a high order model of the control plant that is fitted to identified FRFs. To guarantee robustness, models with varied eigenvalues (according to the expected change) were used for validation of control performance during the design process. Figure 8 shows measured FRFs of the control plant with and without control. The effect of the control can be seen in the significantly reduced resonance amplitude. This results in increased process stability. Without control the process (20000 rpm, 0.15 mm feed per tooth) was only stable up to a depth of cut of 3 mm. Figure 9 shows surfaces of cuts with a depth of cut of 4 mm: without control chatter occurred and with active control the process was stable. The measured orbits of the spindle are shown in Figure 10. (a) shows the stable orbit, caused by the cutting forces. In the unstable case (b) this movement is superposed by the oscillation due to chatter. The stable orbit has a frequency of 666 Hz and the chatter frequency is approx. 530 Hz. The maximum stable depth of cut with active control was 6 mm. This is an improvement in milling performance of 100 % for this case.

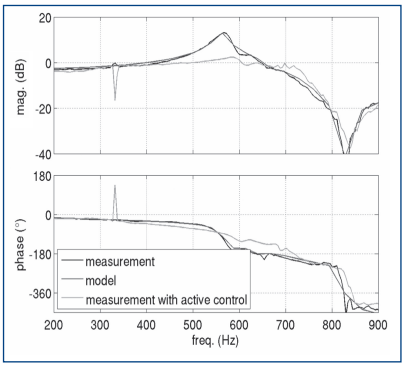

Figure 8. *FRFs of spindle during idle run.*

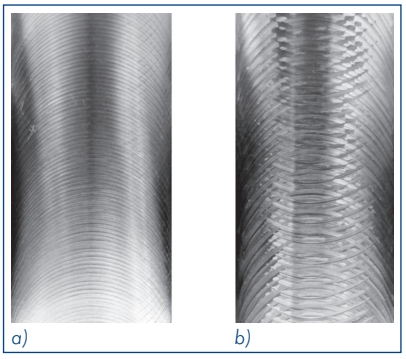

Figure 9. *Workpiece surface: a) Controller on b) Controller off.*

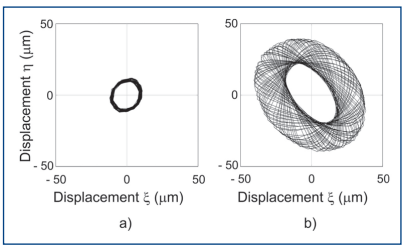

Figure 10. *Measured orbits of the spindle deflection. a) Controller on b) Controller off.*

6. Conclusion

Based on impulse-hammer experiments on a rotating motor spindle a two-degree of freedom model of the milling process is constructed. Using semi-discretization the system dynamics for increasing depth of cut is calculated. The resulting poles in the z-domain are mapped to corresponding poles on the s-plane taking into account aliasing-effect. This shows a change of natural frequency and

damping of the spindle-mechanics with increasing depth of cut before the stability limit is reached. Experimental identification using an electromagnetic actuator that is integrated into the spindle yields the system dynamics during milling. A comparison of theoretical and experimental results shows good conformity. Finally an active-control scheme is presented that allows stable operation at increased depth of cut. Experiments are performed to validate the control performance.

Acknowledgement
This research is supported by the Deutsche Forschungsgemeinschaft (DFG) within the priority program 1156 'Adaptronik für Werkzeugmaschinen'. The authors would like to thank Andreas Schiffler from PTW for his support preparing the test-setup and performing the measurements.

References
[Altintas 1995] Altintas, Y., Budak, E., Analytical Prediction of Stability Lobes in Milling, Annals of the CIRP, Vol. 44, pp. 357-362, 1995,
[Faasen 2007] Faasen, R., Chatter Prediction and Control for High-Speed Milling: Modeling and Experiments, PhD Thesis, TU Eindhoven, Eindhoven, Germany, 2007.
[Ganguli 2005] Ganguli, A., Chatter reduction through active vibration damping, PhD Thesis, Universite Libre De Bruxelles, Belgium, 2005.
[Gradisek 2005] Gradisek, J., Kalveram, M., Inperger, T., Weinert, K., Stépán, G., Govekar, E., Grabec, I., On stability prediction for milling, Int. Journal of Maschine Tools & Manufacture 45, pp. 769-781, 2005.
[Haase 2005] Haase, F., The Investigation and Design of a Piezoelectric Active Vibration Control System for Vertical Machining Centers, School of Computing and Engineering, The University of Huddersfield, United Kingdom, 2005,
[Insperger 2000] Insperger, T., Stépán, G., Stability of the Milling Process, Periodica Polytechnica Ser. Mech. Eng. Vol. 44(1), p. 47-57, 2000.
[Insperger 2002] Insperger, T., Stépán, G., Semi-discretization method for delayed systems, Int. J. Numer. Meth. Engng, Vol. 55, pp. 503-518, 2002.
[Lutz 2003] Lutz, H., Wendt, W., Taschenbuch der Regelungstechnik, 5. ed., Verlag Harry Deutsch, Frankfurt am Main, Germany, 2003.
[Ries 2006] Ries, M., Pankoke, S., Gebert, K., Increase of Material Removal Rate with an Active HSC Milling Spindle, Proc. of the Adaptronic Congress, Germany, 2006.
[Scandella 2004] Scandella, J. S., Les machines-outils s'affranchissent du „broutage", L'Usine Nouvelle, France, 2004.
[Späh 2008] Späh, B., Regelungskonzepte zur aktiven Dämpfung einer hybridgelagerten Motorspindel, Diplomarbeit, Technische Universität Darmstadt, Darmstadt, Germany, 2008.
[Stephens 1996] Stephens, L. S., Knospe, C. R., mu-Synthesis Based, Robust Conroller Design for AMB Machining Spindles, 5th Int. Symp. on Magnetic Bearings, pp.153-158, 1996.
[Weck 2006] Weck, M., Brecher, C., Werkzeugmaschinen 5 – Messtechnische Untersuchung und Beurteilung, dynamische Stabilität, Springer Verlag, Germany, 2006.
[Welch 1967] Welch, P.D, The Use of Fast Fourier Transform for the Estimation of Power Spectra: A Method Based on Time Averaging Over Short, Modified Periodograms, IEEE Trans. Audio Electroacoustics, Vol. AU-15, pp. 70-73,1967.

Contact:
Dipl. Ing. Britta Späh
FG Mechatronik im Maschinenbau, TU Darmstadt
Petersenstr. 30, 642 87 Darmstadt, Germany
tel: +49 615 116 5601, e-mail:spaeh@mim.tu-darmstadt.de